Front. Phys. 10, 107401 (2015)
DOI 10.1007/s11467-014-0446-9

RESEARCH ARTICLE

Quasiparticle scattering interference in the renormalized Hubbard model

Shu-Hua Wang, Huai-Song Zhao, Feng Yuan†

College of Physics, Qingdao University, Qingdao 266071, China

Corresponding author. E-mail: †qdyuanfeng@hotmail.com

Received June 9, 2014; accepted July 31, 2014

In this paper, we study the quasiparticle scattering interference phenomenon in the presence of a single impurity within the renormalized Hubbard model. By calculating the energy and momentum dependence of the Fourier-transformed local density of states in the full Brillouin zone, we can qualitatively describe the main features of the quasiparticle scattering interference phenomenon in cuprate superconductors using a single point-like impurity. In particular, we show that with increasing energy, the position of the peak along the nodal ($[0,0] \rightarrow [\pi,\pi]$) direction moves steadily to a large momentum region, while the position of the peak along the antinodal ($[0,0] \rightarrow [\pi,0]$) direction moves toward the center of the Brillouin zone.

Keywords impurity, renormalized Hubbard model, local density of states, Gutzwiller approximation

PACS numbers 74.62.Dh, 74.20.Mn, 74.25.Bt, 74.20.-z

1 Introduction

The effect of impurity is a fundamental area for the investigation of the unusual physical properties by probing the microscopic electronic structure of unconventional superconductors [1]. In particular, in contrast to conventional superconductors with an s-wave symmetry superconducting (SC) gap, non-magnetic impurities can also produce a strong pair-breaking effect in unconventional superconductors with a non s-wave symmetry SC gap. With the improvements in energy and spatial resolutions, scanning tunneling microscopy (STM) [2] has been used to probe local properties on an atomic scale around the positions of impurity in real space, especially around inhomogeneous electronic structures. STM obtains the local properties of quasiparticles by measuring the tip-sample differential tunneling conductance $g(\boldsymbol{r}, E)$, where $g(\boldsymbol{r}, E)$ is proportional to the local density of states (LDOS) $N(\boldsymbol{r}, E)$ as in [3, 4],

$$g(\boldsymbol{r}, E) \propto N(\boldsymbol{r}, E) \tag{1}$$

Moreover, the momentum-space information of quasiparticles can be obtained by a Fourier transform of the position (r) and the energy-dependent local density of states, $N(\boldsymbol{r}, E)$. Therefore, both real-space and momentum-space modulations of the local density of states are acquired simultaneously [5, 6]. The quasiparticle scattering interference phenomenon characterized by peaks in the local density of states is believed to be an important issue, and includes the physical processes dominating quasiparticle scattering, and quasiparticle momentum-space structure and dispersion [5]. By virtue of systematic studies using STM [5], the energy- and momentum-dependence of the Fourier-transformed local density of state modulations is well established. Local peaks along the antinodal direction ($[0,0] \rightarrow [\pi,0]$) in the full Brillouin zone appear at a finite $\boldsymbol{q}$ at very low energy, and move steadily inward toward the center of the full Brillouin zone. On the other hand, the peaks along the nodal direction ($[0,0] \rightarrow [\pi,\pi]$) appear and move steadily toward larger $\boldsymbol{q}$ with increasing energy. These peaks at well-defined wavevectors $\boldsymbol{q}_i$ obey the Octet model [6]. Theoretically, within the phenomenological d-wave Bardeen-Cooper-Schrieffer (BCS) formalism [7–13], the properties of a quasiparticle and its related quasiparticle scattering interference phenomenon have been studied by considering the effect of impurity. These studies show that a single (or few impurities) in a d-wave superconducting state play a crucial role in explaining the results observed by STM experiments [5, 6]. Moreover, within the framework of the kinetic energy-driven SC mechanism [14–16], the key features of the quasiparticle scattering interference phenomenon in cuprate

superconductors in the SC state are captured by considering a single impurity.

The unconventional physical properties of doped cuprates are mainly attributed to the strong electron correlation in the CuO_2 plane [17] Superconductivity appears at doping concentration $\delta \approx 0.05$ below the SC transition temperature T_c, and have a dominant d-wave symmetry SC gap $\Delta_{\boldsymbol{k}} = \Delta(\cos k_x - \cos k_y)/2$ [18, 19]. With increasing doping concentration, T_c increases in the underdoped region, reaches a maximum in optimal doping, and then decreases in the overdoped region [20] while T^*, depicting the pseudogap phenomenon [21, 22], decreases monotonically in the entire doped region. The interplay between the SC gap and the pseudogap is believed to be crucial to understanding the unusual SC mechanism: in particular, the origin of the pseudogap and its role in the onset of superconductivity. In order to explain the unconventional SC mechanism in cuprate superconductors, a resonant valence bond (RVB) theory using a Gutzwiller projected BCS wave function was proposed by Anderson [23], where the Gutzwiller projector removes all double-occupancy states. Following this, Baskaran, Zou, and Anderson provided a mean field theory [24] and found that T_c is limited to the doping concentration. In particular, a renormalized Hamiltonian approach was proposed by Zhang *et al.* [25], where Gutzwiller renormalization factors were introduced to replace the effect of the projection operator. This theory was developed as a "plain vanilla" theory by Anderson *et al.* [26]. As in Zhang [25], in this paper, we introduce the Gutzwiller renormalization factors into the Hubbard model, establish a self-consistent mean field theory, and calculate the energy- and momentum-dependence of the Fourier-transformed local density of states in the full Brillouin zone.

The characteristic feature of cuprate superconductors is the presence of a two-dimensional (2D) CuO_2 plane. In this case, it is widely accepted that the essential physics of the doped CuO_2 plane is captured by a single-band Hubbard model on a square lattice [23, 27]. In the large U limit, the Hubbard model can be expressed as a t–J model

$$H = -t \sum_{\langle ij\rangle,\sigma} (C^{\dagger}_{i\sigma} C_{j\sigma} + h.c.) + \mu \sum_{i\sigma} C^{\dagger}_{i\sigma} C_{i\sigma} + J \sum_{\langle ij\rangle} (\boldsymbol{S}_i \cdot \boldsymbol{S}_j - \frac{1}{4} n_i n_j), \tag{2}$$

supplemented by an on-site local constraint $\sum_{\sigma} C^{\dagger}_{i\sigma} C_{i\sigma} \leqslant 1$ to avoid double occupancy, where $\sum_{\langle ij\rangle}$ represents summation over the nearest neighbor pairs, $C^{\dagger}_{i\sigma}$ ($C_{i\sigma}$) is the electron creation (annihilation) operator at the lattice site i with spin σ, $\boldsymbol{S}_i = (S^x_i, S^y_i, S^z_i)$ are spin operators at site i, μ is the chemical potential, $n_i = n_{i\uparrow} + n_{i\downarrow}$ is the number of electrons at site i, and $n_{i\sigma} = C^{\dagger}_{i\sigma} C_{i\sigma}$. The strong electron correlation in the CuO_2 plane manifests itself by the on-site local constraint, which is very difficult to solve through an analytic approach. In order to deal with the electron's single-occupancy local constraint in the t–J model (2), a renormalized Hamiltonian approach was proposed by Zhang and others [25, 26], where the Gutzwiller renormalization factors were introduced to rewrite the Hamiltonian. The renormalized Hamiltonian can be expressed as

$$H = -g_t t \sum_{\langle ij\rangle,\sigma} (C^{\dagger}_{i\sigma} C_{j\sigma} + h.c.) + \mu \sum_{i\sigma} C^{\dagger}_{i\sigma} C_{i\sigma} + g_s J \sum_{\langle ij\rangle} (\boldsymbol{S}_i \cdot \boldsymbol{S}_j - \frac{1}{4} n_i n_j), \tag{3}$$

where g_t and g_s are Gutzwiller renormalization factors to modify the kinetic energy and magnetic energy, respectively, and have a simple form by taking into account the strong correlation effect [25, 28],

$$g_t = \frac{2\delta}{1+\delta}, \quad g_s = \frac{4}{(1+\delta)^2}, \tag{4}$$

with the hole concentration $\delta = 1 - n$. According to $S^+_i = C^{\dagger}_{i\uparrow} C_{i\downarrow}, S^z_i = \frac{1}{2}(C^{\dagger}_{i\uparrow} C_{i\uparrow} - C^{\dagger}_{i\downarrow} C_{i\downarrow})$ and the singlet creation operator

$$b^{\dagger}_{ij} = \frac{1}{\sqrt{2}} (C^{\dagger}_{i\uparrow} C^{\dagger}_{j\downarrow} - C^{\dagger}_{i\downarrow} C^{\dagger}_{j\uparrow}), \tag{5}$$

the t–J model (3) can be rewritten as

$$H = -g_t t \sum_{\langle ij\rangle,\sigma} (C^{\dagger}_{i\sigma} C_{j\sigma} + h.c.) - g_s J \sum_{\langle ij\rangle} b^{\dagger}_{ij} b_{ij}. \tag{6}$$

Within the mean field approximation, the Hamiltonian can be obtained in momentum space as

$$H = \sum_{\boldsymbol{k},\sigma} (\xi_{\boldsymbol{k}} - \mu) C^{\dagger}_{\boldsymbol{k}\sigma} C_{\boldsymbol{k}\sigma} - 2 g_s J \sum_{\boldsymbol{k}} \Delta \gamma^{(d)}_{\boldsymbol{k}} (C_{\boldsymbol{k}\downarrow} C_{-\boldsymbol{k}\uparrow} + C^{\dagger}_{-\boldsymbol{k}\uparrow} C^{\dagger}_{\boldsymbol{k}\downarrow}), \tag{7}$$

where $\xi_{\boldsymbol{k}} = -\frac{1}{2}(2 g_t t + p g_s J) Z \gamma_{\boldsymbol{k}}$, Z is the number of nearest neighbor sites on a square lattice, the self-consistent order parameters $\Delta = \sqrt{2}\langle b_{ij}\rangle$ (the magnitude of the d-wave gap), $p = \langle C^{\dagger}_{i\sigma} C_{j\sigma}\rangle$, $\gamma_{\boldsymbol{k}} = \frac{1}{2}(\cos k_x + \cos k_y)$, $\gamma^{(d)}_{\boldsymbol{k}} = \frac{1}{2}(\cos k_x - \cos k_y)$. In this case, we define the electron diagonal and off-diagonal Green's functions as

$$G(\boldsymbol{k}, \tau - \tau') = -\langle T C_{\boldsymbol{k}\sigma}(\tau) C^{\dagger}_{\boldsymbol{k}\sigma}(\tau')\rangle,$$

$$\Gamma^{\dagger}(\boldsymbol{k},\tau-\tau^{'})=-\langle TC^{\dagger}_{-\boldsymbol{k}\uparrow}(\tau)C^{\dagger}_{\boldsymbol{k}\downarrow}(\tau^{'})\rangle. \tag{8}$$

From Eq. (7), we can obtain the mean field electron diagonal and off-diagonal Green's functions in BCS type [29, 30]:

$$G(\boldsymbol{k},\omega)=\frac{U^2_{\boldsymbol{k}}}{\omega-E_{\boldsymbol{k}}}+\frac{V^2_{\boldsymbol{k}}}{\omega+E_{\boldsymbol{k}}}, \tag{9a}$$

$$\Gamma^{\dagger}(\boldsymbol{k},\omega)=\frac{g_{\rm s}J\Delta\gamma^{(d)}_{\boldsymbol{k}}}{E_{\boldsymbol{k}}}(\frac{1}{\omega-E_{\boldsymbol{k}}}-\frac{1}{\omega+E_{\boldsymbol{k}}}), \tag{9b}$$

where $U^2_{\boldsymbol{k}}=[1+(\xi_{\boldsymbol{k}}-\mu)/E_{\boldsymbol{k}}]/2$, $V^2_{\boldsymbol{k}}=[1-(\xi_{\boldsymbol{k}}-\mu)/E_{\boldsymbol{k}}]/2$, and the quasiparticle spectrum $E_{\boldsymbol{k}}=\sqrt{(\xi_{\boldsymbol{k}}-\mu)^2+(2g_{\rm s}J\Delta\gamma^{(d)}_{\boldsymbol{k}})^2}$. Thus, we get the self-consistent equations

$$\delta=\frac{1}{N}\sum_{\boldsymbol{k}}\frac{\xi_{\boldsymbol{k}}-\mu}{E_{\boldsymbol{k}}}\tanh\frac{1}{2}\beta E_{\boldsymbol{k}}, \tag{10a}$$

$$1=\frac{2}{N}\sum_{\boldsymbol{k}}\frac{g_{\rm s}J(\gamma^{(d)}_{\boldsymbol{k}})^2}{E_{\boldsymbol{k}}}\tanh\frac{1}{2}\beta E_{\boldsymbol{k}}, \tag{10b}$$

$$p=\frac{1}{2N}\sum_{\boldsymbol{k}}\gamma_{\boldsymbol{k}}\left[1-\frac{\xi_{\boldsymbol{k}}-\mu}{E_{\boldsymbol{k}}}\tanh\frac{1}{2}\beta E_{\boldsymbol{k}}\right]. \tag{10c}$$

Then, the self-consistent parameters δ and p, and the chemical potential μ are determined by self-consistent calculation. In this sense, our results are controllable without using adjustable parameters. In particular, the self-consistent parameter Δ describing the magnitude of the d-wave gap is not the superconducting order parameter but the pseudogap, whereas the superconducting order parameter $\Delta_{\rm SC}$ can be obtained by the Gutzwiller method [25],

$$\Delta_{\rm SC}=g_{\rm t}\Delta. \tag{11}$$

In this case, $T_{\rm c}\propto g_{\rm t}\Delta$, and can be understood by the work of Lee and Wen [31], where the SC state is destroyed by the thermal excitation of only the low-lying quasiparticles, leaving the large energy gap intact in underdoped cuprate, and $T_{\rm c}$ is proportional to δ (then the superfluid density). Many anomalous physical properties of cuprate superconductors is the result of a combination of the large d-wave gap and low superfluid density.

In cuprate superconductors, although the values of J and t are believed to vary somewhat from compound to compound [32,33], the commonly used parameters in this paper are chosen as $t/J=5$ for qualitative discussion. We calculated the doping dependence of the self-consistent parameter (Δ) (solid line) and the superconducting order parameter ($\Delta_{\rm SC}$) (dashed line), and plotted the results of Δ and $\Delta_{\rm SC}$ as a function of doping for temperature $T=0.002J$ in Fig. 1.

Our results show that Δ (then the pseudogap) smoothly decreases with increasing doping concentration

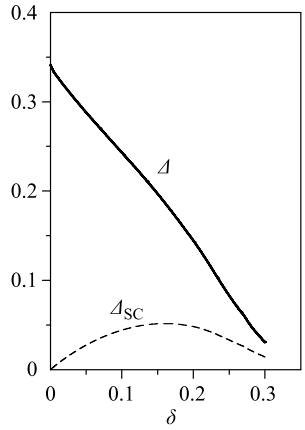

Fig. 1 The self-consistent parameter (Δ) (*solid line*) and superconducting order parameter ($\Delta_{\rm SC}$) (*dashed line*) as functions of doping for temperature $T=0.002J$ with parameter $t/J=5.0$.

in the entire doping range from an underdoped to a heavily overdoped regime. However, in contrast to the case of Δ in the underdoped regime, $\Delta_{\rm SC}$ vanishes near $\delta=0$, increases with increasing doping concentration in the underdoped regime, reaches a maximum in the optimal doping, and then decreases with increasing doping in the overdoped regime. Therefore, the superconducting order is controlled by the d-wave gap and the renormalization factor, which explains the doping dependence of the $T_{\rm c}$. In particular, the renormalization factor is closely related to the quasiparticle coherent weight [34–36].

For the convenience of the following discussions, the full electron Green's function, including the electron diagonal and off-diagonal Green's functions (9), can be expressed in Nambu representation as

$$\tilde{G}(\boldsymbol{k},\omega)=\begin{pmatrix} G(\boldsymbol{k},\omega),\Gamma(\boldsymbol{k},\omega) \\ \Gamma^{\dagger}(\boldsymbol{k},\omega),-G(\boldsymbol{k},-\omega)\end{pmatrix}, \tag{12}$$

$$\tilde{G}(\boldsymbol{k},\omega)=\frac{\omega\tau_0+(\xi_{\boldsymbol{k}}-\mu)\tau_3+2g_{\rm s}J\Delta\gamma^{(d)}_{\boldsymbol{k}}\tau_1}{\omega^2-E^2_{\boldsymbol{k}}}, \tag{13}$$

where τ_0 is a unit matrix, τ_1 and τ_3 are Pauli matrices, and the tilde in this paper denotes a Nambu space matrix.

In the presence of a single point-like impurity, the scattering potential can be written as

$$\tilde{V}=V_0\delta(\boldsymbol{r})\tau_3. \tag{14}$$

Then, the full electron Green's function with the impurity scattering contribution described by the T matrix [1] in real space can be represented as

$$\tilde{G}_{\rm I}(\boldsymbol{r},\boldsymbol{r}',\omega)=\tilde{G}(\boldsymbol{r}-\boldsymbol{r}',\omega)+\tilde{G}(\boldsymbol{r},\omega)\tilde{T}(\omega)\tilde{G}(-\boldsymbol{r}',\omega) \tag{15}$$

where the T matrix can be obtained as [1]

$$\tilde{T}(\omega) = \frac{V_0\tau_3}{1-\tilde{G}(\omega)V_0\tau_3}, \tag{16}$$

$$\tilde{T}(\omega) = \frac{1}{[1-G(\omega)V_0][1-G(-\omega)V_0]} \times \begin{pmatrix} V_0[1-G(-\omega)V_0], 0 \\ 0, -V_0[1-G(\omega)V_0] \end{pmatrix} \tag{17}$$

with

$$G(\omega) = \frac{1}{N}\sum_{\boldsymbol{k}y} G(\boldsymbol{k},\omega). \tag{18}$$

In this case, the T matrix is a diagonal matrix, and the elements of the off-diagonal matrix vanish because the mean value of the gap function $\Delta\gamma_{\boldsymbol{k}}^{(d)}$ in Fermi surface is zero. The position-dependence of the local density of states can be obtained as

$$N(\boldsymbol{r},\omega) = -\frac{1}{\pi}\mathrm{Im}\tilde{G}_I(\boldsymbol{r},\omega) = N_0(\omega) + \delta N(\boldsymbol{r},\omega), \tag{19}$$

where $N_0(\omega)$ is the homogeneous density of states in the pure system, reflecting a homogeneous background, whereas the second term $\delta N(\boldsymbol{r},\omega)$ is the modulation for the homogeneous density of states due to the single point-like impurity scattering potential. From Eq. (15), this can be expressed as

$$\delta N(\boldsymbol{r},\omega) = -\frac{1}{\pi}\mathrm{Im}[\tilde{G}(\boldsymbol{r},\omega)\tilde{T}(\omega)\tilde{G}(-\boldsymbol{r},\omega)]_{11} \tag{20}$$

Then, the Fourier-transformed local density of states can be obtained as

$$\delta N(\boldsymbol{q},\omega) = -\frac{1}{\pi}\mathrm{Im}\left(\frac{1}{N}\sum_{\boldsymbol{k}}[\tilde{G}(\boldsymbol{k}+\boldsymbol{q},\omega)\tilde{T}(\omega)\tilde{G}(\boldsymbol{k},\omega)]_{11}\right). \tag{21}$$

We now begin to discuss the quasiparticle scattering interference phenomenon in cuprate superconductors, and choose parameter $t/J = 5$ in this paper, as mentioned above. In this case, the Fourier-transformed local density of states $\delta N(\boldsymbol{q},\omega)$ in Eq. (21) as functions of energy and momentum are evaluated, and the results of $|\delta N(\boldsymbol{q},\omega)|$ with energy (a) $\omega = -0.2J$, (b) $\omega = -0.4J$, (c) $\omega = -0.6J$, and (d) $\omega = -0.8J$ at temperature $T = 0.002J$ for doping concentration $\delta = 0.15$ in the presence of single point-like impurity potential scatterer of strength $V = 0.5J$ are plotted in Fig. 3.

As we can see, the results of $|\delta N(\boldsymbol{q},\omega)|$ are fourfold

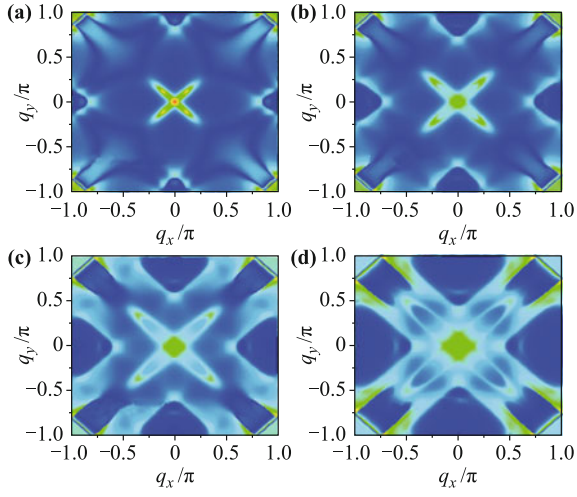

Fig. 2 The Fourier-transformed local density of states as a function of momentum in the full Brillouin zone with energy **(a)** $\omega = -0.2J$, **(b)** $\omega = -0.4J$, **(c)** $\omega = -0.6J$, and **(d)** $\omega = -0.8J$ at temperature $T = 0.002J$ for doping concentration $\delta = 0.15$ in the presence of single point-like potential scatterer of strength $V = 0.5J$.

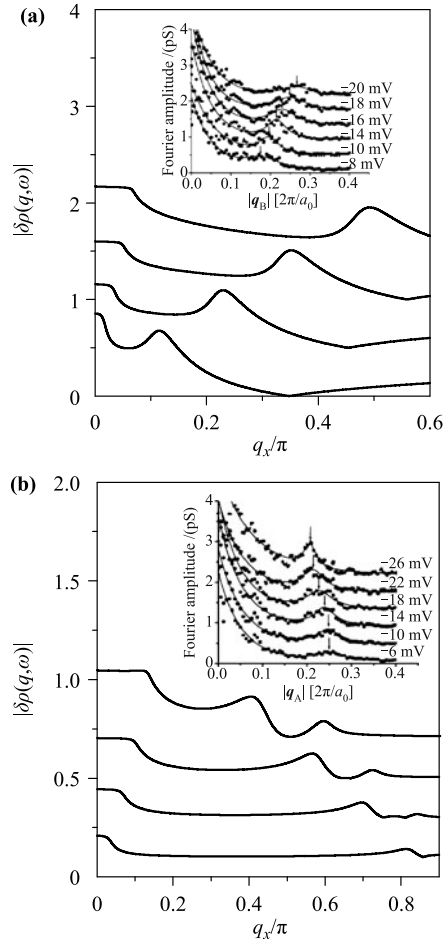

Fig. 3 The Fourier-transformed local density of states as a function of momentum along the **(a)** nodal direction ($[0,0] \to [\pi,\pi]$) and **(b)** antinodal direction ($[0,0] \to [\pi,0]$) with energy $\omega = -0.2J$, $\omega = -0.4J$, $\omega = -0.6J$, and $\omega = -0.8J$ (from bottom to top) at temperature $T = 0.002J$ for doping concentration $\delta = 0.15$ in the presence of a single point-like potential scatterer of strength $V = 0.5J$. *Inset*: the corresponding experimental results of cuprate superconductors taken from Ref. [5].

symmetric, and some local peaks (bright region) appear at different wavevectors $\boldsymbol{q}$ predicted by the Octet model [5]. These local peaks in momentum space are closely related to the intensity of the modulation for local density states as a result of the presence of point-like impurity potential. Moreover, the positions of these local peaks in momentum space change rapidly with increasing energy, particularly the local peaks whose wavevectors $\boldsymbol{q}$ along the nodal direction ($[0,0] \rightarrow [\pi,\pi]$) and the antinodal direction ($[0,0] \rightarrow [\pi,0]$) are often investigated. To show these points clearly, we carried out a series of calculations for the momentum-dependence of $\delta N(\boldsymbol{q},\omega)$ with increasing energy, and the results of $|\delta N(\boldsymbol{q},\omega)|$ as a function of wavevector $\boldsymbol{q}$ in momentum space along the (a) nodal direction ($[0,0] \rightarrow [\pi,\pi]$) and the (b) antinodal direction ($[0,0] \rightarrow [\pi,0]$) with energy $\omega = -0.2J$, $\omega = -0.4J$, $\omega = -0.6J$, and $\omega = -0.8J$ (from bottom to top) at temperature $T = 0.002J$ for doping concentration $\delta = 0.15$ in the presence of single point-like potential scatterer of strength $V = 0.5J$, are plotted in Fig. 4. For comparison, the corresponding STM experimental data of $Ba_2Sr_2CaCu_2O_{8+\delta}$ [5] is also shown in Fig. 4 (inset).

We can see that the local peak along the nodal direction in momentum space (wavevector $\boldsymbol{q}$) changes rapidly and intricately with energy, and appears and moves steadily to large $\boldsymbol{q}$ with increasing energy. On the other hand, the peak with the wavevector $\boldsymbol{q}$ oriented towards the antinodal direction appears at finite $|\boldsymbol{q}|$ at very low energy ($|\omega|$), and moves steadily inwards toward $[0,0]$ (the center of the full Brilliouin zone), in qualitative agreement with STM experimental data [5, 6]. Moreover, we extracted the dispersion of local peaks according to the energy-dependence of the peaks in Fig. 4, and plotted the results of the positions of the peaks in $|\delta N(\boldsymbol{q},\omega)|$ as a function of energy along the (a) $[0,0] \rightarrow [\pi,\pi]$ (nodal) direction and the (b) $[0,0] \rightarrow [\pi,0]$ (antinodal) direction for temperature $T = 0.002J$ at doping concentration $\delta = 0.15$, in the presence of a single point-like potential scatterer of strength $V = 0.5J$ in Fig. 4 in comparison with the corresponding experimental data [5] of $Ba_2Sr_2CaCu_2O_{8+\delta}$ (inset).

Our results clearly show that the position of the local peak along the nodal direction ($[0,0] \rightarrow [\pi,\pi]$) decreases monotonically with decreasing energy ($|\omega|$). In the antinodal direction ($[0,0] \rightarrow [\pi,0]$) on the other hand, the position of the peak increases monotonically with decreasing energy ($|\omega|$). All these results are in qualitative agreement with those observed from STM experimental measurement [5] on $Ba_2Sr_2CaCu_2O_{8+\delta}$.

The essential physics of the energy- and momentum-dependence of quasiparticle scattering interference in cuprate superconductors can be attributed to the d-wave

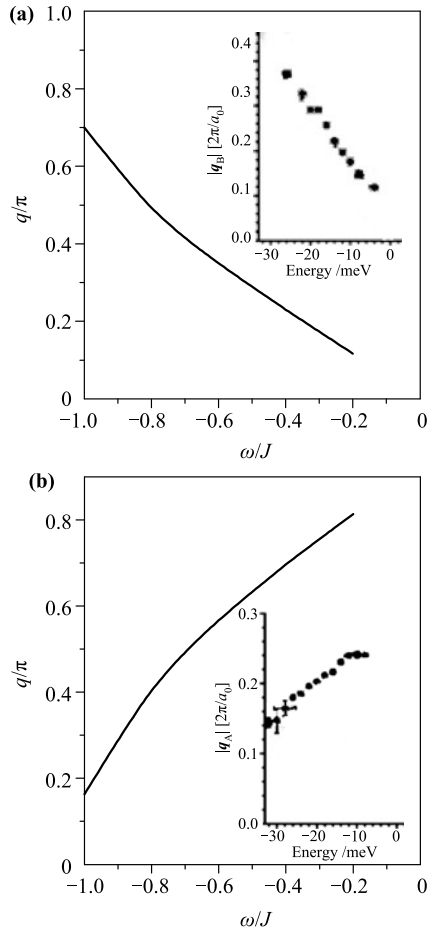

Fig. 4 The Fourier-transformed local density of states as a function of momentum along the **(a)** nodal direction ($[0,0] \rightarrow [\pi,\pi]$) and **(b)** antinodal direction ($[0,0] \rightarrow [\pi,0]$) with energy $\omega = -0.2J$, $\omega = -0.4J$, $\omega = -0.6J$, and $\omega = -0.8J$ (from bottom to top) at temperature $T = 0.002J$ for doping concentration $\delta = 0.15$ in the presence of a single point-like potential scatterer of strength $V = 0.5J$. Inset: the corresponding experimental results of cuprate superconductors taken from Ref. [5].

symmetry gap in the presence of a single point-like impurity. There is a gapless excitation of the quasiparticle as a result of the existence of nodes in the d-wave symmetry gap. The impurity can then induce a finite density of quasiparticle excitations even at zero temperature [37], and these quasiparticles induced by impurity can then be scattered by the impurity. From Eq. (9), we see that the quasiparticle dispersion in the renormalized mean field theory based on the Hubbard model is a simple d-wave BCS formalism:

$$E_{\boldsymbol{k}} = \sqrt{(\xi_{\boldsymbol{k}} - \mu)^2 + \Delta_{\boldsymbol{k}y}^2} \tag{22}$$

where $\Delta_{\boldsymbol{k}} = \Delta_0 \gamma_{\boldsymbol{k}}^{(d)}$ describes the k-dependent magnitude of the energy gap at the Fermi surface, with $\Delta_0 = 2g_s J\Delta$, and for $\delta = 0.15$ and $\Delta_0 \approx 1.2J$. The Bogoliubov quasiparticle dispersion E_k in cuprate

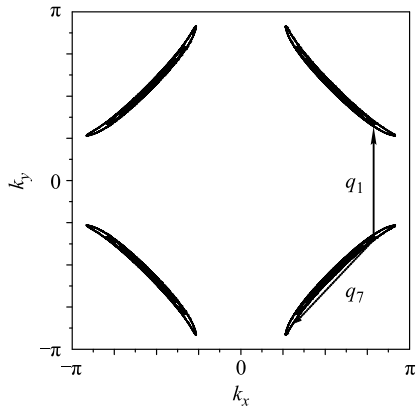

Fig. 5 Schematic plot of the "banana-shaped" contours of constant energy (CCE) in the first Brillouin zone. The modulation of wave vectors q_1, q_7 indicates the antinodal and nodal elastic scattering processes discussed in this paper, respectively.

superconductors has "banana-shaped" closed contours of constant energy (CCE) surrounding the d-wave nodes in Fig. 5, in qualitative agreement with those observed from the experimental measurement of angle-resolved photoemission spectroscopy (ARPES) [38, 39]. Then, for given energy ω, it causes local maxima to appear in the density of states at the eight banana tips $k_i(\omega)$ obeying the Octet model [6]. Moreover, with increasing energy ($|\omega|$), the size of the banana-shaped quasiparticle contours of constant energy (CCE) increases. Therefore, the magnitude of the characteristic wavevector along the antinodal direction (then q_1 in the Octet model) decreases. Then, the position of the lowest-energy peak along the antinodal direction in the Fourier-transformed local density of states moves steadily inward toward the center of the full Brillouin zone. By contrast, in the nodal direction, the magnitude of the characteristic wavevector (then q_7 in the Octet model) increases with increasing energy ($|\omega|$), because of which the position of the peak moves steadily toward the large momentum.

In conclusion, on the one hand, we have established a renormalized mean field theory in the Hubbard model by replacing the on-site electron single-occupancy constraint with two renormalization factors. We have shown that the self-consistent gap parameter decreases almost linearly upon increasing doping concentration, whereas the superconducting gap shows a dome-like doping dependence. On the other hand, we studied the quasiparticle scattering interference phenomenon observed in cuprate superconductors within the renormalized mean field theory based on the Hubbard model. We showed that the quasiparticle scattering interference pattern in the presence of a single point-like impurity is strongly energy dependent because of the dominant d-wave symmetry gap. In particular, with increasing energy, the positions of the peaks along different high-symmetry directions in the Brillouin zone exhibit completely different momentum-dependence. The positions of the peak along the nodal direction ($[0,0] \rightarrow [\pi,\pi]$) decreases monotonically with decreasing energy ($|\omega|$), while in the antinodal direction ($[0,0] \rightarrow [\pi,0]$), the position of the peak increases monotonically with decreasing energy ($|\omega|$). Our current theoretical results qualitatively capture the main features of the quasiparticle scattering interference phenomenon observed by STM experiments in cuprate superconductors [5], hence showing that the quasiparticle scattering interference phenomenon is very closely related to the presence of impurity.

Acknowledgements This work was supported by the National Natural Science Foundation of China under Grant No. 10774082.

References

1. A. V. Balatsky, I. Vekhter, and J.-X. Zhu, Impurity-induced states in conventional and unconventional superconductors, *Rev. Mod. Phys.* 78(2), 373 (2006)
2. O. Fischer, M. Kugler, I. Maggio-Aprile, C. Berthod, and C. Renner, Scanning tunneling spectroscopy of high-temperature superconductors, *Rev. Mod. Phys.* 79(1), 353 (2007)
3. T. Hanaguri, Y. Kohsaka, J. C. Davis, C. Lupien, I. Yamada, M. Azuma, M. Takano, K. Ohishi, M. Ono, and H. Takagi, Quasiparticle interference and superconducting gap in $Ca_{2-x}Na_xCuO_2Cl_2$, *Nature Physics* 3(12), 865 (2007)
4. I. M. Vishik, E. A. Nowadnick, W. S. Lee, Z. X. Shen, B. Moritz, T. P. Devereaux, K. Tanaka, T. Sasagawa, and T. Fujii, A momentum-dependent perspective on quasiparticle interference in $Bi_2Sr_2CaCu_2O_{8+\delta}$, *Nature Physics* 5(10), 718 (2009)
5. J. E. Hoffman, K. McElroy, D.-H. Lee, K. M. Lang, H. Eisaki, S. Uchida, and J. C. Davis, Imaging quasiparticle interference in $Bi_2Sr_2CaCu_2O_{8+\delta}$, *Science* 297(5584), 1148 (2002)
6. K. McElroy, R. W. Simmonds, J. E. Hoffman, D.-H. Lee, J. Orenstein, H. Eisaki, S. Uchida, and J. C. Davis, Relating atomic-scale electronic phenomena to wave-like quasiparticle states in superconducting $Bi_2Sr_2CaCu_2O_{8+\delta}$, *Nature* 422(6932), 592 (2003)
7. Q.-H. Wang and D.-H. Lee, Quasiparticle scattering interference in high-temperature superconductors, *Phys. Rev. B* 67(2), 020511 (2003)
8. D. Zhang and C. S. Ting, Energy-dependent modulations in the local density of states of the cuprate superconductors, *Phys. Rev. B* 67(10), 100506 (2003)
9. L.-Y. Zhu, W. A. Atkinson, and P. J. Hirschfeld, Power spectrum of many impurities in a d-wave superconductor, *Phys. Rev. B* 69(6), 060503 (2004)

10. T. S. Nunner, W. Chen, B. M. Andersen, A. Melikyan, and P. J. Hirschfeld, Fourier transform spectroscopy of d-wave quasiparticles in the presence of atomic scale pairing disorder, *Phys. Rev. B* 73(10), 104511 (2006)
11. B. Liu, X. Yan, and F. Yuan, Electron correlation and impurity-induced quasiparticle resonance states in cuprate superconductors, *Journal of the Physical Society of Japan* 82(10), 114713 (2013)
12. B. Liu, X. Yan, and F. Yuan, Quasiparticle resonance states induced by a nonmagnetic impurity in Gossamer superconductors, *Solid State Communications* 177, 123 (2014)
13. Z. P. Huang, X. X. Wan, and F. Yuan, Local density of states around two nonmagnetic impurities in cuprate superconductors, *Front. Phys.* 6(3), 309 (2011)
14. S. P. Feng, Kinetic energy driven superconductivity in doped cuprates, *Phys. Rev. B* 68(18), 184501 (2003)
15. S. P. Feng, T. X. Ma, and H. M. Guo, Magnetic nature of superconductivity in doped cuprates, *Physica C* 436(1), 14 (2006)
16. Z. Wang, B. Liu, and S. P. Feng, Extinction of quasiparticle scattering interference in cuprate superconductors, *Phys. Lett. A* 374(30), 3084 (2010)
17. M. A. Kastner, R. J. Birgeneau, G. Shirane, and Y. Endoh, Magnetic, transport, and optical properties of monolayer copper oxides, *Rev. Mod. Phys.* 70(3), 897 (1998)
18. C. C. Tsuei and J. R. Kirtley, Pairing symmetry in cuprate superconductors, *Rev. Mod. Phys.* 72(4), 969 (2000)
19. H. Ding, M. R. Norman, J. C. Campuzano, M. Randeria, A. F. Bellman, T. Yokoya, T. Takahashi, T. Mochiku, and K. Kadowaki, Angle-resolved photoemission spectroscopy study of the superconducting gap anisotropy in $Bi_2Sr_2CaCu_2O_{8+x}$, *Phys. Rev. B* 54(14), R9678 (1996)
20. J. L. Talion, C. Bernhard, H. Shaked, R. L. Hitterman, and J. D. Jorgensen, Generic superconducting phase behavior in high-T_c cuprates: T_c variation with hole concentration in $YBa_2Cu_3O_{7-\delta}$, *Phys. Rev. B* 51(18), 12911 (1995)
21. T. Timusk and B. Statt, The pseudogap in high-temperature superconductors: An experimental survey, *Rep. Prog. Phys.* 62(1), 61 (1999)
22. S. Hüfner, M. A. Hossain, A. Damascelli, and G. A. Sawatzky, Two gaps make a high-temperature superconductor? *Rep. Prog. Phys.* 71(6), 062501 (2008)
23. P. W. Anderson, The resonating valence bond state in La_2CuO_4 and superconductivity, *Science* 235(4793), 1196 (1987)
24. G. Baskaran, Z. Zou, and P. W. Anderson, The resonating valence bond state and high-T_c superconductivity — A mean field theory, *Solid State Communications* 63(11), 973 (1987)
25. F. C. Zhang, C. Gros, T. M. Rice, and H. Shiba, A renormalised Hamiltonian approach to a resonant valence bond wavefunction, *Supercond. Sci. Technol.* 1(1), 36 (1988)
26. P. W. Anderson, P. A. Lee, M. Randeria, T. M. Rice, N. Trivedi, and F. C. Zhang, The physics behind high-temperature superconducting cuprates: The "plain vanilla" version of RVB, *J. Phys.: Condens. Matter* 16(24), R755 (2004)
27. F. C. Zhang and T. M. Rice, Effective Hamiltonian for the superconducting Cu oxides, *Phys. Rev. B* 37(7), 3759 (1988)
28. F. C. Zhang, Gossamer superconductor, Mott insulator, and resonating valence bond state in correlated electron systems, *Phys. Rev. Lett.* 90(20), 207002 (2003)
29. J. Bardeen, L. N. Cooper, and J. R. Schrieffer, Theory of superconductivity, *Phys. Rev.* 108(5), 1175 (1957)
30. J. R. Schrieffer, Theory of superconductivity, San Francisco: Addison-Wesley, 1964
31. P. A. Lee and X.-G. Wen, Unusual superconducting state of underdoped cuprates, *Phys. Rev. Lett.* 78(21), 4111 (1997)
32. Mark S. Hybertsen, E. B. Stechel, W. M. C. Foulkes, and M. Schlüter, Model for low-energy electronic states probed by X-ray absorption in high-T_c cuprates, *Phys. Rev. B* 45(17), 10032 (1992)
33. A. Damascelli, Z. Hussain, and Z.-X. Shen, Angle-resolved photoemission studies of the cuprate superconductors, *Rev. Mod. Phys.* 75(2), 473 (2003)
34. Kai-Yu Yang, C. T. Shih, C. P. Chou, S. M. Huang, T. K. Lee, T. Xiang, and F. C. Zhang, Low-energy physical properties of high-T_c superconducting Cu oxides: A comparison between the resonating valence bond and experiments, *Phys. Rev. B* 73(22), 224513 (2006)
35. H. Ding, J. R. Engelbrecht, Z. Wang, J. C. Campuzano, S.-C. Wang, H.-B. Yang, R. Rogan, T. Takahashi, K. Kadowaki, and D. G. Hinks, Coherent quasiparticle weight and its connection to high-T_c superconductivity from angle-resolved photoemission, *Phys. Rev. Lett.* 87(22), 227001 (2001)
36. T. Yoshida, X. J. Zhou, T. Sasagawa, W. L. Yang, P. V. Bogdanov, A. Lanzara, Z. Hussain, T. Mizokawa, A. Fujimori, H. Eisaki, Z.-X. Shen, T. Kakeshita, and S. Uchida, Metallic behavior of lightly doped $La_{2-x}Sr_xCuO_4$ with a fermi surface forming an arc, *Phys. Rev. Lett.* 91(2), 027001 (2003)
37. A. C. Durst and P. A. Lee, Impurity-induced quasiparticle transport and universal-limit Wiedemann–Franz violation in d-wave superconductors, *Phys. Rev. B* 62(2), 1270 (2000)
38. U. Chatterjee, M. Shi, A. Kaminski, A. Kanigel, H. M. Fretwell, K. Terashima, T. Takahashi, S. Rosenkranz, Z. Z. Li, H. Raffy, A. Santander-Syro, K. Kadowaki, M. R. Norman, M. Randeria, and J. C. Campuzano, Nondispersive Fermi arcs and the absence of charge ordering in the pseudogap phase of $Bi_2Sr_2CaCu_2O_{8+\delta}$, *Phys. Rev. Lett.* 96(10), 107006 (2006)
39. U. Chatterjee, M. Shi, A. Kaminski, A. Kanigel, H. M. Fretwell, K. Terashima, T. Takahashi, S. Rosenkranz, Z. Z. Li, H. Raffy, A. Santander-Syro, K. Kadowaki, M. Randeria, M. R. Norman, and J. C. Campuzano, Anomalous dispersion in the autocorrelation of angle-resolved photoemission spectra of high-temperature $Bi_2Sr_2CaCu_2O_{8+\delta}$ superconductors, *Phys. Rev. B* 76(1), 012504 (2007)